Characterising the discharge cycle of $CaCl_2$ and $LiNO_3$ hydrated salts within a vermiculite composite scaffold for thermochemical storage

R.J. Sutton, E. Jewell, J. Elvins, J.R. Searle and P. Jones

Corresponding author : Dr Eifion Jewell, e.jewell@swansea.ac.uk

1- Swansea University, College of Engineering, Bay Campus, Fabian Way. Crymlyn Burrows, Swansea, SA1 8EN, 437543@swansea.ac.uk, e.jewell@swansea.ac.uk

Keywords

Thermochemical storage, salt hydration, transpired solar collector, Composite sorbents Calcium Chloride, Lithium Nitrate

Abstract

Transpired solar collectors (TSC) are an efficient means of building heating but due to the demand / use mismatch their capabilities are maximised when paired with a suitable storage technology. The hydration and / dehydration of inorganic salts provides an appropriate energy storage medium which is compatible with the air temperature provided by a conventional TSC (<70 °C). The study reports on the technical appraisal of materials which are compatible with building scale energy storage installations. Two salts ($CaCl_2$, and $LiNO_3$) were impregnated into porous vermiculite to form a salt in matrix (SIM). Their performance during the discharge portion of the cycle at high packing density was examined using a laboratory scale reactor. Reactor and exit temperature increases were considerably lower than those predicted from first principles. Peak reactor temperature rises of only 14 °C were observed with a reduction in temperature output from this initial peak over 60 hours. Poor salt utilization resulting from deliquescence near the reactor inlet was identified as being the source of the reduced performance. Changes in reactor size, orientation and cycling between input periods of moist and dry air did not improve reactor performance. The investigation has identified that moist air transit through the packed SIM reactor column is limited to approximately 100 mm from the air inlet. This has implications for reactor design and the operation of any practical building scale installation. Predictions of building scale energy storage capabilities based on simple scaling of laboratory tests under estimate considerably the volume and complexity of equipment required.

1. Introduction

Building scale inter seasonal thermal energy storage provides a means of balancing excess solar derived thermal energy over the summer months with winter demand [1]. One solution for harvesting energy during summer months is a transpired solar collector (TSC). A solar energy absorbing material is coated to a perforated surface which forms the exterior of the building cladding and the air drawn through and over the surface experiences an uplift in temperature as convective energy transfer occurs between the high temperature surface and the air [2]. This technology is readily implemented at building scale and commercial products for this are available [3,4]. A limitation of TSC technology is that it often provides thermal input when there is little

demand and vice versa. This supply / demand mismatch varies both daily and seasonally. Intra day or inter seasonal storage would provide a significant additional benefit to both the uptake to TSC and thus to building energy management in general. The principle of operation of such a system is shown in Figure 1. During dry warm periods (Figure 1a) , the hot air produced by the TSC can be used to chemically change the storage material and this air can then be safely discharged to the exterior of the building. During colder periods, Figure 1b, the cold air can be elevated in temperature by chemical reactions in the thermochemical storage and supplied directly to the building or as input air with a temperature uplift to a conventional air heating system.

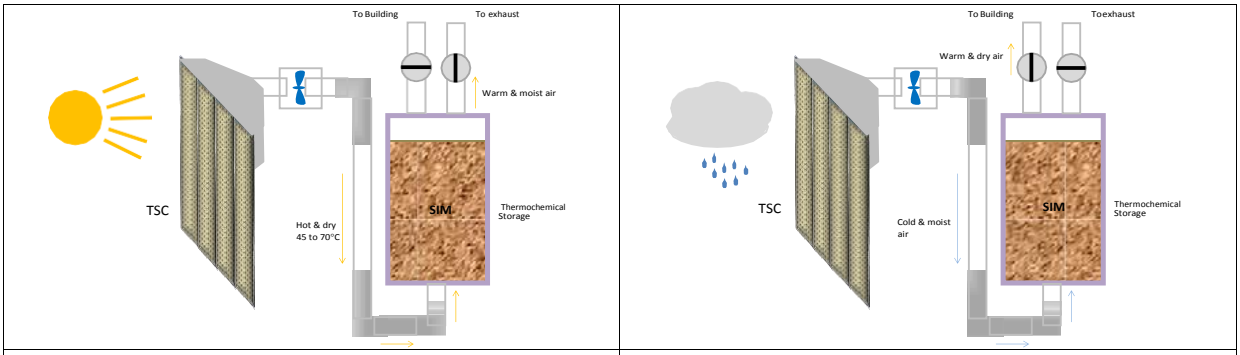

(a) Storage during warm weather | (b) Discharge during cold weather

Figure 1 : Simplified schematic of charge and discharge stages of the thermochemical cycle using TSC for building thermal storage and heating.

The maximum air temperature which can be obtained in Northern European conditions during summer months from a TSC are typically 70 °C with mean air temperatures of approximately 45 °C [5]. These operational temperature limits govern the most suitable chemical storage mechanism. Chemical storage through the hydration / dehydration of salts potentially provides an efficient means of storing energy as high energy densities can potentially be achieved [6–9], material costs are low, chemicals are non toxic and non flammable and the choice of salt can be matched to the operational temperature window available. The storage and release of thermal energy is via the fully reversible endothermic /exothermic chemical reaction:
$salt \cdot x(H_2O) + heat \leftrightarrow salt + x(H_2O)$ [10]. A number of candidate salt materials are available [9,11,12] and hosting these salts within porous matrices (SIMs) have been shown to have minimum hysteresis and material degradation over hydration and dehydration cycles [13]. The porous matrix also provides a robust material which can be readily handled and can provide a large internal area where vapour / salt hydration / dehydration can occur [11,8].

The choice of porous matrix is driven by the need to provide a stable, non-reactive, porous, safe, abundant and cheap material with a large potential surface area where salt could be deposited, [11,14]. Past studies have examined thermochemical storage potential of a range of hygroscopic chemical salts impregnated into a range of porous host matrices including vermiculite, activated carbon pellets, zeolites and silica Gel[15,16]. Casey et al [13,17] studied comprehensively characterised a variety of salts and matrices but did so with 1.5L of material thinly and uniformly distributed over a wire mesh (a layer thickness of 10 – 15 mm) within a large reactor (90 litres) effectively a storage density of approximately 0.03 GJ/m^3. This is significantly lower than the energy density would be required for a building. The flow, mass transfer and thermal transfer through a larger porous bulk will likely be significantly different from that experienced through a thin layer

which is of the order of 2 – 8 particles thick, [18]. Zhu et al [15] examined a larger (40Kg) rig containing silica gel / $CaCl_2$ SIM and obtained peak exit temperatures of around 40 °C providing an energy density of 1 kJ/ g (0.806 GJ/m^3) at a salt : matrix ratio of approximately 0.5. There is potential to further increases this storage capacity by an increase in the salt : matrix proportion, although silica gel itself provides a storage mechanism through adsorption[19]. Given the limited number of studies which have examined the SIM materials at high density then there is a danger that simple scaling of the results from lab to building scale presents are misleading

For a given salt, the practical storage density limit of SIM technology is potentially increased by increasing the salt content and by providing a thick and dense media through which the moist air is passed. There is a dearth of published literature on the energy release from a reactor where there is a thick (>50 mm) layer of SIM through which the moist air must pass. Thus, the primary objective of the study was to establish the discharge characteristics when used at a storage density (i.e. tightly packed) which is compatible with building storage at a high salt : matrix ratio. Understanding the behaviour of these storage media at a high density is critical in determining whether it is a suitable material for building scale applications. The SIM behaviour influences reactor designs, space allocation, operational overheads, and overall suitability for building thermal storage. The study was initiated (and influenced) a development programme installing a 5 ton storage system as a retrofit to an industrial building [20].

2. Method

2.1 Materials

$CaCl_2$ and $LiNO_3$, were selected as chemical salts as they are well studied and their change in hydration states lie within the expected 10 – 80 °C temperature window, [17,21–23]. The relative merits of these materials are summarised in terms of theoretical storage potential of the selected salts, using low temperature heat from a solar thermal collector in Table 1. This storage potential was calculated from the dehydration temperatures of the hydrated states of the salt, and the change in enthalpy associated with the change in hydrated state [24]. Of the two materials $CaCl_2$ provides a more attractive commercial proposition as it is significantly cheaper and therefore provides a more economic solution but the LiNO3 provides a potentially denser energy storage capacity.

Table 1: Relative merits of the salts investigated in matrix form used in investigation.

	CaCl2	LiNO3
Hydration states (Assuming dehydration @ >60°C)	.2H_2O to . 4H_2O .4H_2O to . 6H_2O	$LiNO_3$ to $LiNO_3$.3H_2O
Potential heat of hydration, (0 – 60°C) KJ/mole	1204	757
Solubility (g/100g of H_2O) @ 20°C	74.5	52.2
Approximate relative cost £/Kg	1	10
Mass : Vermiculite ratio @ 50% volume	2	1.9
Mass of H_2O required for 1g salt to fully hydrate	0.494	0.61
Theoretical energy Density of SIM (GJ/m^3)	1.30	1.65

The host matrix chosen for this study was vermiculite as this had been shown to meet the main requirements for an inert matrix upon which the salt can be deposited. It is widely available mineral which contain aluminium-iron-magnesium silicates in various proportions depending on source [25]. It is an porous multi lamella structured material which has applications in protective packaging, horticulture, and fire proofing has also been considered as matrix for cooling applications[26]. The inter lamella gaps provide an area which can be filled with the active salt to form a vermiculite / salt composite [25,27].

The choice of ratio of inert matrix to salt in the SIM requires a balance of thermodynamic efficiency, which dictates higher salt content and practical needs where a low salt content is preferred. These practical limitations are associated with the elimination of unattached salt crystals, prevention of deliquescence, utilization of the salt and the free air path through a macro porous structure of individual particles. The ratios used were calculated based on 50% mean free volume of the vermiculite as reported in the literature [13,17]. The choice of 50% of the available volume was made as full liquid penetration of all the internal void space (as measured by gas absorption) by a liquid was not deemed to be realistic. Initial experimentation with the $CaCl_2$ material found that solid mass ratios above 2:1 produced a SIM with properties which were not considered to be beneficial to performance. In comparison to the 2:1 SIM (Figure 2 a), an excess build-up of salt is evident on the surface of the 3:1 SIM (Figure 2 b). These loosely bound salt crystal tended to be removed during handling to produce a mixture of larger SIM particles and smaller dust size crystals of salt, Figure 1 (d). In contrast the 2:1 SIM produced a uniform distribution of salt impregnated particles, Figure 1(c). In addition, there was evidence that some vermiculite particles were cleaved apart by the quantity of salt between the lamella. This further reduced the mean particle size, producing a more dust particles in the media.

(a) 2:1 $CaCl_2$: Vermiculite SIM (image width = 6.5 mm)

(b) 3:1 $CaCl_2$: Vermiculite SIM (image width = 6.5 mm)

(c) 2:1 $CaCl_2$: Vermiculite SIM as bulk mixture | (d) 3:1 $CaCl_2$: Vermiculite SIM as bulk mixture.

Figure 2 : Images of the $CaCl_2$ SIM material as prepared at (a) 2:1 Salt : vermiculite ratios used and (b) 3:1 salt : vermiculite ratio.

A saturated salt solution was created and this was mixed with the vermiculite host matrix using a continuous spraying and slow agitation of the vermiculite. This slow agitation ensured complete mixing of the vermiculite and salt solution without physical damage to vermiculite. Samples were subsequently dried in an oven at 120 °C in order remove excess moisture and to elevate each to a hydration state of $CaCl_2.2H_2O$ and $LiNO_3$. Although this temperature is above that which is likely to be experienced during subsequent charging cycles, this ensured the removal of water at a suitable rate while being below that temperature of the next hydration state (where applicable). Each material was made in 2Kg batches to limit uncertainties associated with variability in the vermiculite and processing between batches.

In order to validate that the salt had fully impregnated the core of the vermiculite, EDS (Electron Dispersive Spectroscopy) was carried out on a random selection of particles. These were cleaved in a direction parallel to the lamella and were mounted in a Hitachi TM3000 Desktop SEM and analysed using a Oxford instruments EDS system which allows structural images and elemental mapping of the particle interior. Analysis of the vermiculite grains impregnated with $CaCl_2$ shows that salt solution has fully been absorbed into the centre of the vermiculite, Figure 3, with evidence of both chlorine and calcium throughout the vermiculite particle; with a background oxygen, silicon magnesium and aluminium from the vermiculite. This result was consistent throughout the size range of the particles. Although, EDS provides more qualitative than quantitative measurements, this clearly illustrates that salt has impregnated evenly the entire porous structure of the vermiculite. It was not possible to confirm the same behaviour with the $LiNO_3$ as the Lithium low atomic mass makes detection unreliable.

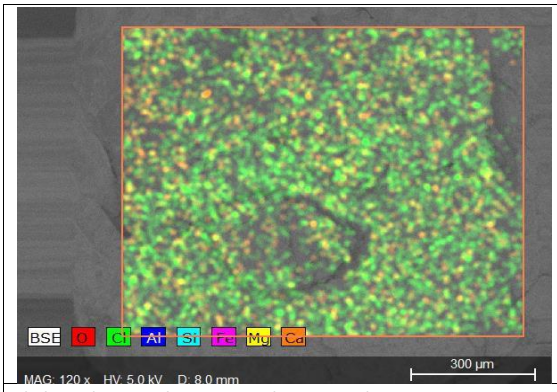

(a) Cl (green) and Ca (Orange) distribution in a smaple particle

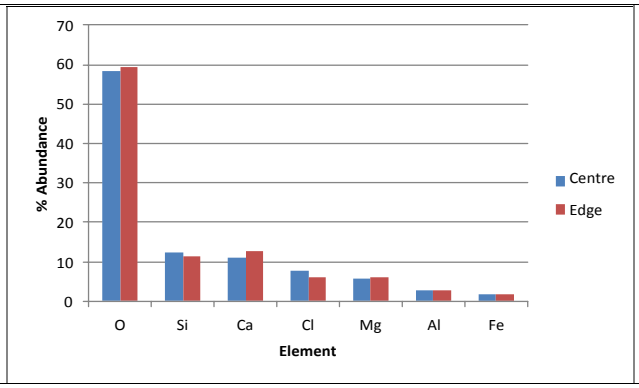

(b) Mean elemental quantities at the edge and centre of particles.

Figure 3 : (a) EDS image and (b) analysis of cross sections at the centre and edge of an individual SIM particle.

Under moisture diffusion conditions the natural absorption capabilities of each salt / vermiculite system was established. The mass of the SIMs were monitored periodically over 150 hrs in environments of varying relative humidity, at temperatures of 20°C ± 1°C. The overall mass increase was related to the number of water molecules gained per molecule of salt, Figure 4. Both $CaCl_2$ and $LiNO_3$ SIM materials exhibit excellent moisture adsorption capabilities at a range of humidity, indicating good potential release of energy, however there are practical limitations associated with the control of moisture adsorption, preventing the dissolution of salt. Even at a moderately low relative humidity, both materials rapidly absorb an excess of moisture. This is not beneficial for heat generation as this additional moisture does not release energy, adds to the thermal mass and reduces the SIM temperature through enthalpy of condensation.

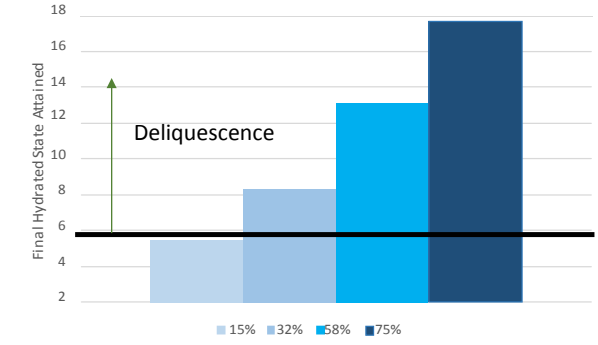

(a) $CaCl_2$

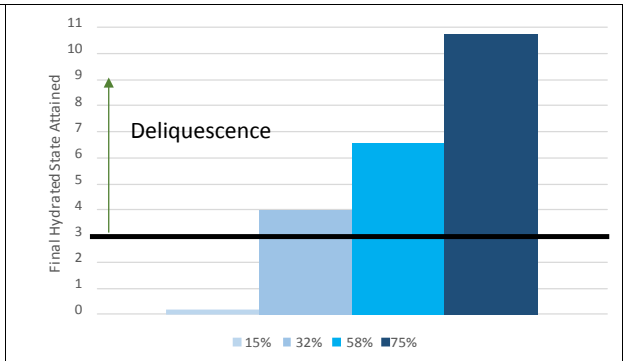

(b) $LiNO_3$

Figure 4 : The final hydrated state attained for the 3 SIMs under diffusion moisture conditions for 4 humidity levels for (a); $CaCl_2$, and (b) $LiNO_3$. The solid line indicates the maximum hydrated state available before salt deliquescence.

2.2 Experimental setup

In order to simulate the discharge hydration portion of the cycle (replicating Figure 1 b) experimental apparatus was created whereby controlled humidity air could be passed through a reactor column of SIM, Figure 5. Temperature and humidity were monitored prior to entrance and exit of the reactor as well as at 3 points along the reactor path.

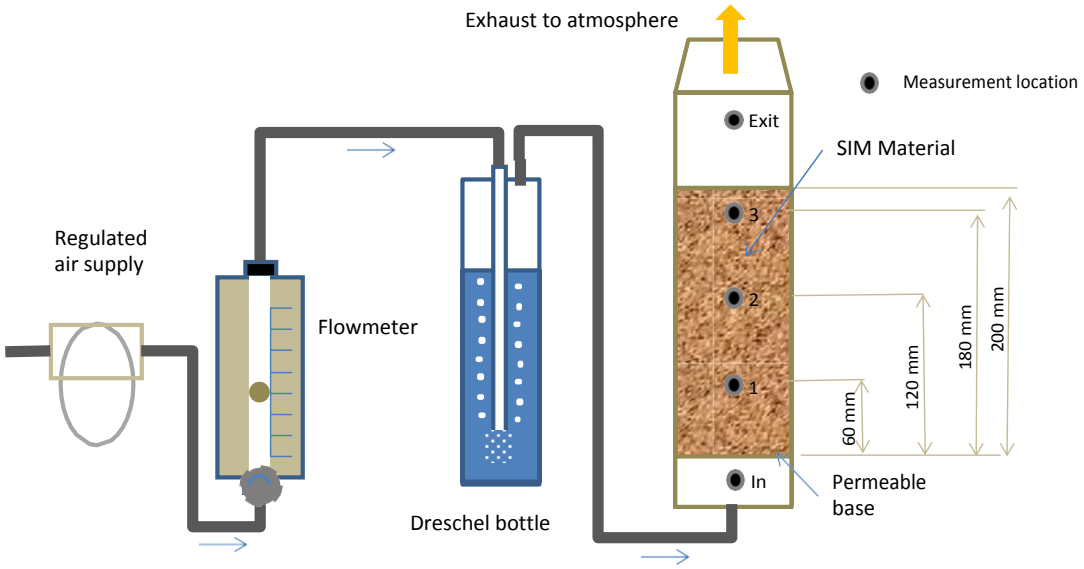

Figure 5: Schematic of the experimental apparatus developed to investigate parameters representative of a typical thermal storage system.

Air at 20°C and 75% relative humidity was generated by passing oil free compressed air through a sintered porous glass block in a 5 litre Dreschel bottle of DI water. This provided inlet air at 19 °C containing 12.9 gH_2O / m^3 . Although this inlet temperature is above that which could be expected during UK winter months (typically -5°C – 15 °C), the moisture content corresponds to maximum possible moisture loading at 15 °C and therefore represents the maximum delivery rate of reactant to the reactor. Air flow rate was controlled independently upstream of the Dreschel bottle and consistent humidity could be obtained independent of the air flow rate. The reactor diameter was 60 mm and volume of the reactor was 570 cm^3 . It was consistently filled to contain 125 g of material, based on the salt: vermiculite ratio of 2:1. Measurement position 3 corresponded to the fill level of the reactor with the sensor just submerged in the SIM. The temperature was measured using type K thermocouples while measurement of relative humidity was carried out using TE-HPP805C031 sensors. Through repeated measurements of the reactor without SIM, the input temperature could be controlled to within an accuracy of +/- 0.7 C and the relative humidity to within +/- 1 %.

After initial explanatory studies, the reactor was run for 60 hours at 5 l/min at an input moisture level of 12.9 g H_2O/m^3 . This equates to around 5 times the water required to fully hydrate the mass of SIM. This was deemed a practical timescale which would allow full utilization of the SIM and therefore cover a full discharge cycle. Prior to operating with the SIM material, the system was evaluated with dry vermiculite, Figure 6, in order to establish the interactions between the vermiculite and the moisture. There is a little interaction between the incoming water vapour and the vermiculite in the first two hours but for the remaining 18 hours, the moisture level in the reactor remains more or less constant. The fluctuations are associated with minor variations in the in incoming pressurised air. It can therefore be concluded that subsequent variations in water vapour temperature and temperature are primarily a result of salt – water vapour interactions.

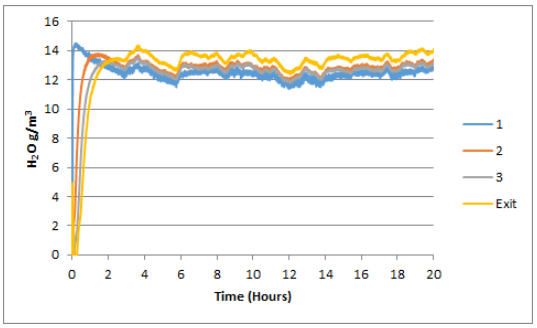

Figure 6 : Reactor air moisture profile for the reactor loaded with dry vermiculite only.

3. Results

3.1 Material discharge characteristics under standard conditions

There is a significant difference between the response of each SIM material and thus each will be presented in turn, prior to a discussion on a comparison of their performance. The overall trends observed are in line with those observed in previous experimental [13,15] and numerical studies [28].

A typical response for the $CaCl_2$ SIM at a flow rate of 5 L/minute is shown in Figure 7(a). At this flow rate the idealised minimum time to hydrate the salt (without deliquescence and assuming there is perfect utilization of the salt) is around 11 hours. Any reduction in the local moisture level below the inlet level shows that water is being absorbed by the SIM and there will be a complimentary increase in local temperature as a result of the enthalpy of formation of the hydrated salt.

Both time and the position within the reactor have a significant effect of the temperature and moisture profiles experienced within the reactor. At the reactor inlet, there is an initial peak in temperature within the first hour, Figure 7(a-iv), and a depression in the water vapour content as the water vapour reacts with the salt. The temperature rise reduces gradually over the next 5 hours and then there is a sudden reduction in temperature and a corresponding increase in water vapour level. This is followed by a more gradual rate of temperature change and a more gradual rate of water vapour level. Beyond 15 hours, the temperature reduces further and there is a increase in moisture level until it stabilises near the input moisture level. Possible mechanism for this temperature profile are explained in the discussion.

As time proceeds, the position of the peak temperature moves up through the reactor, Figure 7(a-iii) and Figure 7(a-ii) indicating a salt – water vapour reaction at each location, although the magnitude of the temperature rise reduces from around 25°C at position 1 to 19 °C at position 2 and 14 °C at position 3. At all positions, the peak temperature occurs prior to an increase in moisture level at the location evidence that the salt – water vapour reaction reaches a peak prior to a situation where there is a local excess of moisture. The temperature rises observed in the reactor core do not immediately result in an increase in the reactor exit temperature with exit temperature rise reaching a peak of around 10 °C some 5 hours after the peak temperature seen at the inlet SIM material. The energy liberated by the hydration reaction on the SIM is therefore not immediately transferred downstream by the air.

With the exception of the inlet, the moisture content in the air remains plateaued at around half the level of inlet moisture content, i.e. there is insufficient moisture available to maintain the a sufficiently high reaction rate of the hydration process and this results in a gradual reduction in temperature. Given that sufficient moisture is being supplied to the reactor, but does not reach a location where it is required, then there must some mechanism where the moisture is prevented from passing through the SIM. Visually a line could be observed moving up through the reactor column, indicating material which was dry and yet to react and that where water was presented and a reaction had taken place, Figure 8. The measurements and visual observations would therefore suggest that the region near the inlet continues to gather moisture from the air although this does process does not liberate energy, i.e. the salt has entered a state of deliquescence. This has several detrimental effects on the performance. The formation of excess water on the SIM surface blocks the passage of the air through the SIM by blocking the intra particle pores. This excess water also readily harvests the moisture from the inlet air reducing the quantity of water vapour which is available for reaction further downstream of the saturated SIM.

The latent heat of vaporization also acts as a sink in the energy balance and reduces the temperatures possible. Finally, the additional water adds to the thermal mass of the system. This phenomena has not been reported previously but has a potentially dramatic effect on the potential application of the technology as it limits operational performance significantly. Essentially, there is insufficient mixing of the moist air with the salt in the reactor which leads to poor salt utilization and the subsequent generation of low temperature lifts. From the position of the sensors and observations, the limit of permeation of moisture through a column of $CaCl_2$ SIM is around 100 mm. Beyond a SIM thickness of 100 mm, any upstream SIM will tend to scavenge moisture and starve the downstream salt / water energy liberating reaction. This will have an impact on future reactor design.

The salt used significantly changes the thermal response of the reactor, although there are some similarities and patterns which are replicated between them, Figure 7(b). With $LiNO_3$ (idealised time to hydration 13 hours) there is an initial spike in temperature at all points in the reactor of between 15°C and 20 °C, but this rapidly reduces to 5°C – 10°C in less than an hour. To coincide with the drop in temperature, there is a rapid increase in the free moisture in the air. The single step of energy liberation of hydration for $LiNO_3$ allows a mechanism for this behaviour to be proposed. It is proposed that the $LiNO_3$ has been rapidly hydrated (liberating the energy) on the surface of the SIM and continues to liberate energy at a far slower rate as the salt within the core of the vermiculite particle is hydrated. As with the $CaCl_2$, there is deliquescence as the moisture level in the air does not reach the level of the input air, indicating that moisture is absorbed to the SIM surface without any energy liberation benefit. In contrast with the $CaCl_2$ behaviour there is no evidence of a lag as one proceeds through the reactor with the peak temperature occurring immediately upon exposure to moist air. The inference that can be drawn by the relative performance of the two materials and its subsequent understanding of the impact on the mechanisms of hydration and energy release are presented in the discussion.

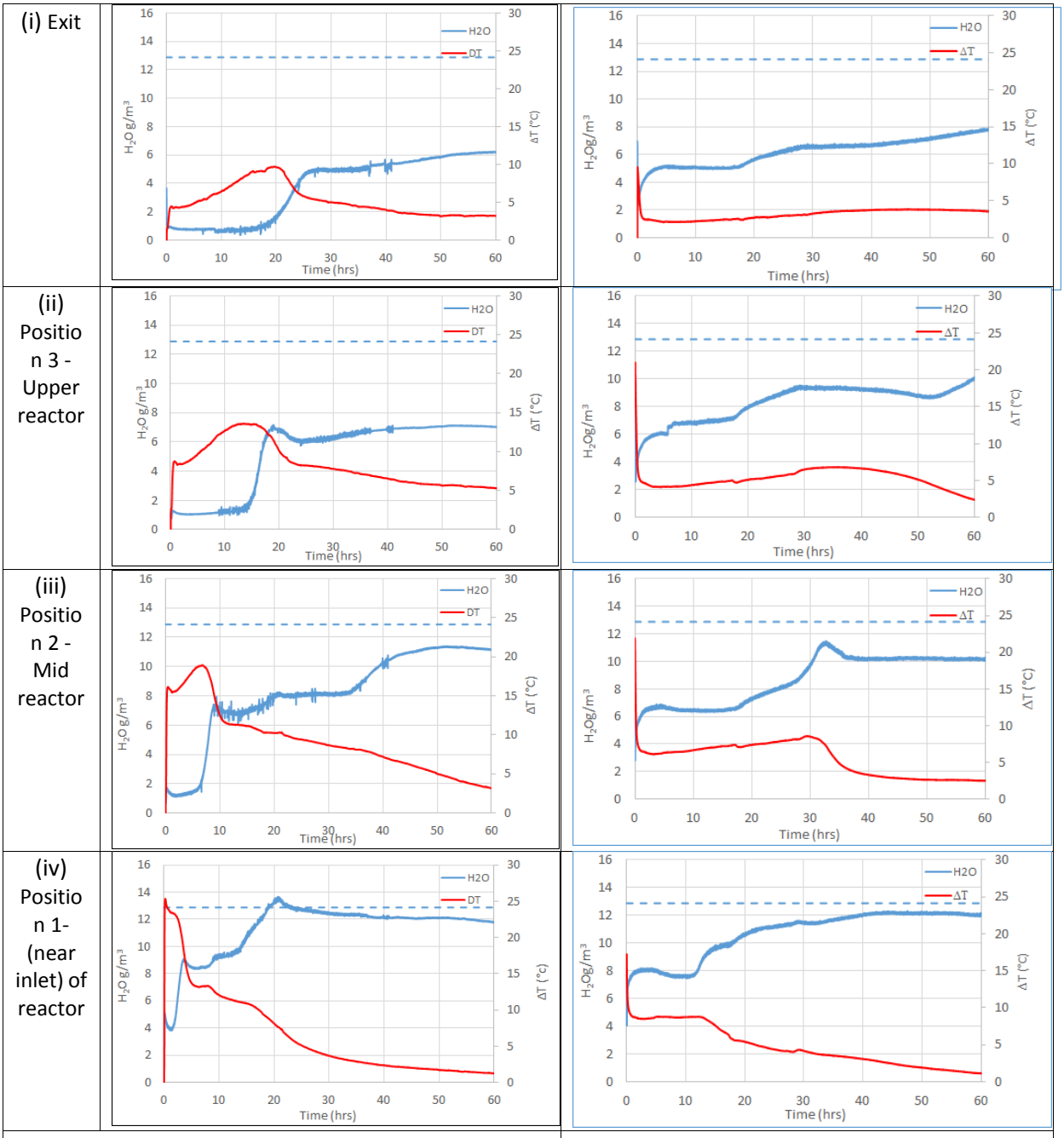

Figure 7: Humidity and ΔT response of SIM through the reactor under the flow of humid air at 5 lpm and inlet water content of 12.9 g H_2O/m^3 (dashed line)

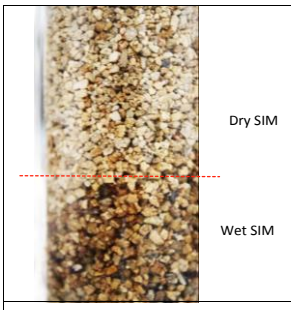

Figure 8 : View of the reactor column, with a line demarking differences in local moisture level at each vertical position.

The measured exit temperatures were significantly lower than those predicted from first principles (Annexe 1), Table 2. Predicted mean exit temperatures uplifts of 29 °C and 30 °C for the $CaCl_2$ and $LiNO_3$ compare with actual mean exit temperature rises of 5.2°C and 3.2 °C respectively. By comparing the total energy stored and that which is obtained at the exit of the reactor, it is possible to calculate an effective discharge utilization. For the vermiculite $CaCl_2$ SIM, only 18 % of the energy stored is released to produce a useful thermal uplift in the air exiting the reactor. For the vermiculite - $LiNO_3$, this reduces to 11%.

Table 2. Predicted and measured

	Vermiculite - $CaCl_2$	Vermiculite - $LiNO_3$
Predicted mean temperature (°C)	29	30
Measured mean temperature	5.2	3.2
Effective discharge utilization %	18%	11%
Effective energy density (GJ/m^3)	0.234	0.182

One possible reason for the low storage utilization and the discrepancy between the predicted and measured mean temperatures was initially attributed with the small size of the reactor. The inherent large surface area (heat transfer surface) to volume ratio which would tend to increase energy loss from the reactor body. This factor combined with the relative mass of the sensors and reactor body which acted as a heat sink on the small reactor material would result in a lower then expected temperature rise.

3.2 Scaled large reactor

A larger reactor was subsequently created (total SIM mass of 700 g, 125 mm diameter) from an lower thermal conductivity material and the experiment repeated at the a comparable salt : water moist air flow rate of 28 L/min. The mean temperatures with the larger reactor showed no improvement in the performance and in most instances produced lower temperature rises than those produced with the smaller reactor, Table 3. The similarity of the behaviour for measurement position at the base and near the the top of the SIM is evident in Figure 9. There is a difference of around 5°C in the initial peak temperature for both SIM materials at the base of the reactor which can be associated with time taken for the moisture to permeate to the greater surface of the from the single inlet on the centreline. This reactor size variant showed that the poor performance could not be attributed to large reactor surface area / volume.

Table 3 : Mean temperature rise and effective utilization over a 60 period for both SIM materials in a 125g and 700 g reactor

	$CaCl_2$		$LiNO_3$	
ΔT °C	125 g reactor	700 g reactor	125 g reactor	700 g reactor
Utilization %				
Exit	5.2	6.4	3.2	1.2
3 – Upper reactor	8.3	7.8	5.3	2.4
2 – Mid reactor	9.2	7.8	5.4	5.2
1 – Reactor bottom	6.5	7.5	4.7	5.9

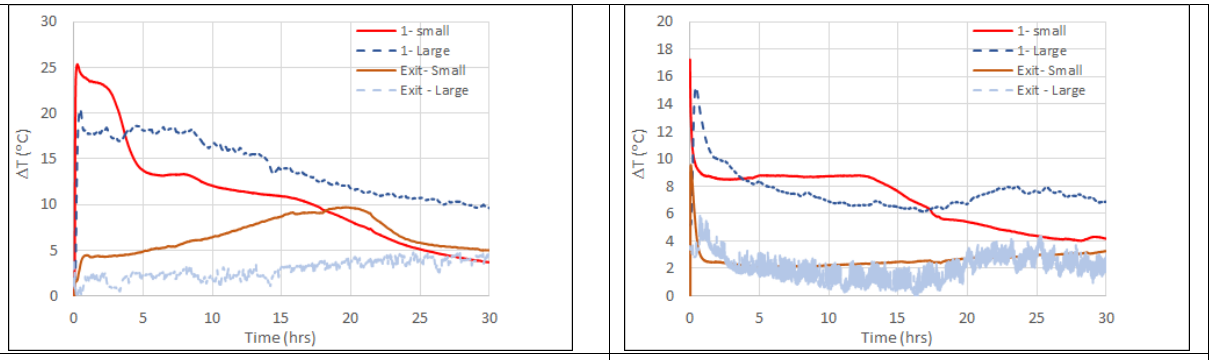

(a) $CaCl_2$ (b) $LiNO_3$

Figure 9 : Temperature profiles for the $CaCl_2$ and $LiNO_3$ in a small (125 g) and large (700 g) reactor at a position (1) bottom and (3) top of the SIM mixture in the reactor

A reduction in the salt matrix ratio may be one way in which the deliquescence could be eliminated but this will have a direct effect on the achievable storage energy density. In order to maintain the high-energy density, alternative approaches to the operation of the reactor which aimed to redistribute the air through the reactor were investigated. Each method was investigated with the $CaCl_2$ SIM as this yielded a steadier temperature evolution during the test and therefore provided a test which could be more readily tested in the laboratory.

3.3 Reactor orientation

The simplest means of changing the flow regime within the reactor was by reactor operation by rotating the reactor by 180° such that moist air entered from the top with the exhaust placed at the bottom of the reactor. In this way, it was anticipated that gravity could aid the transfer of excess water through the reactor column. The orientation of the inlet has an appreciable effect on the temperature and air moisture distribution through the reactor, although the overall mean temperatures are largely reduced over the test period, Figure 10. At the inlet, Figure 10(iii), there is a small reduction in the initial temperature spike, but the remainder of the temperature profile closely follow each other. No conclusive benefits can therefore be drawn from the operation of the reactor with the moist air inlet at the top of the reactor.

(i) Position 3 – Furthest from inlet

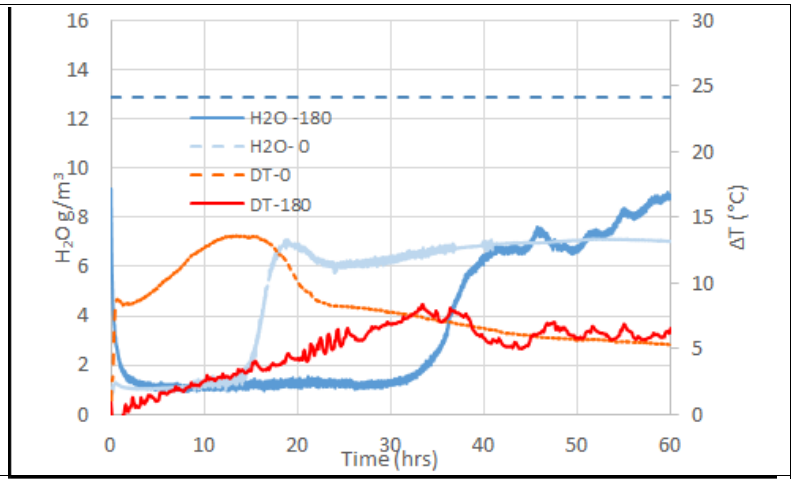

(ii) Position 2 - Mid reactor

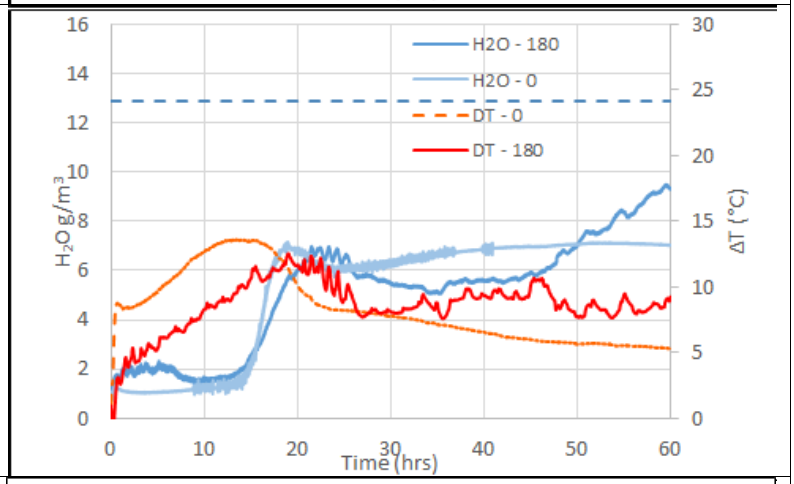

(iii) Position 1- near inlet of reactor

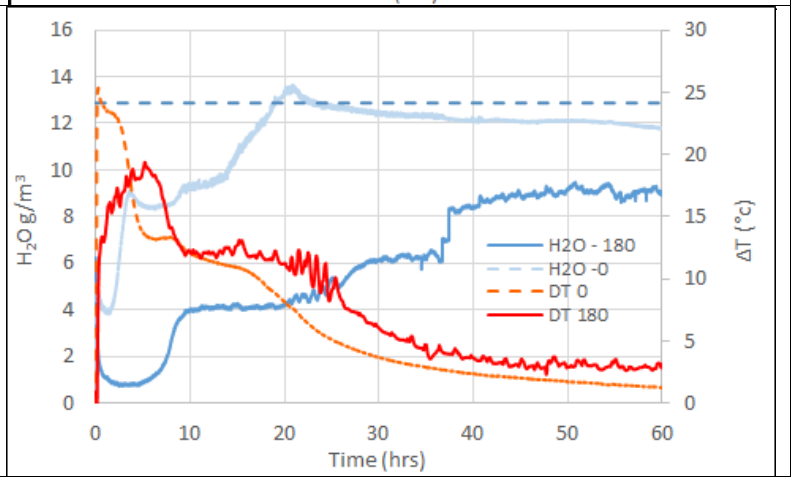

Figure 10 : Temperature and moisture profiles through the reactor for 2 orientations (0 degrees – entry at bottom and 180 degrees – entry from top) of the reactor for the small reactor $CaCl_2$ material at 5 lpm.

3.4 Input air cycling

As no benefits could be identified from position of the inlet, the concept of air cycling was investigated to improve utilization of the salt in the reactor. The concept was based on the hypothesis that by cycling dry and moist air, any excess moisture which had deposited on the surface of the SIM during the moist portion of the cycle would re-evaporate during the dry air portion of the cycle and be transported further into the reactor to react with the un-hydrated SIM further

downstream. The investigation examined the proportion of wet : dry air supplied in a 2 hour cycle. During the moist air portion of the cycle energy is liberated (with a subsequent increase in temperature) while during the dry air portion of the cycle, there is a reduction in temperature rise as the air passes through reactor without liberating energy from the SIM, Figure 10. In each case, there is negative temperature rise in the bulk (relative to the inlet air) as there is some evaporative cooling effect. The evaporation of the excess water (or water which has not been hydrated into the salt structure) from the SIM results in a lowering of the SIM temperature beyond the inlet air temperature. This evaporation is also evident in the moisture levels which are maintained within the reactor even when dry air traverses through the reactor. The air cycling reduces the overall level of moisture in the bottom of the reactor (Figure 11 (iii and iv), this does not result in any discernible increase in temperature in the reactor. Irrespective of the moist air:dry air ratio, the net effect of the temperature developed within the reactor is negligible with each cycling mode more or less following the standard operation. Cycling air inlet moisture levels therefore have no beneficial effect on the reactor performance.

(i) Exit	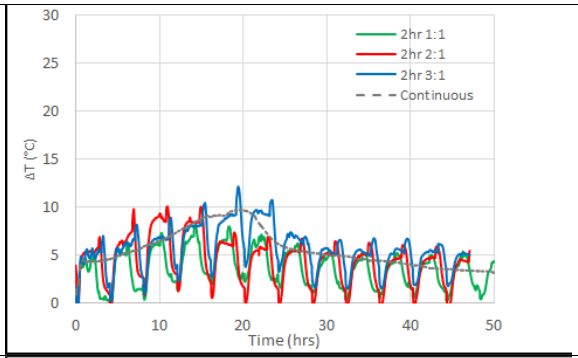	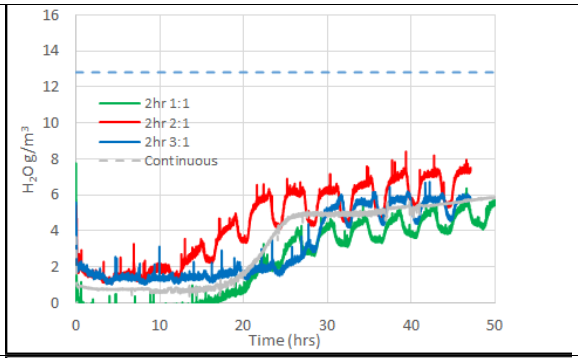
(ii) Position 3 - Upper reactor	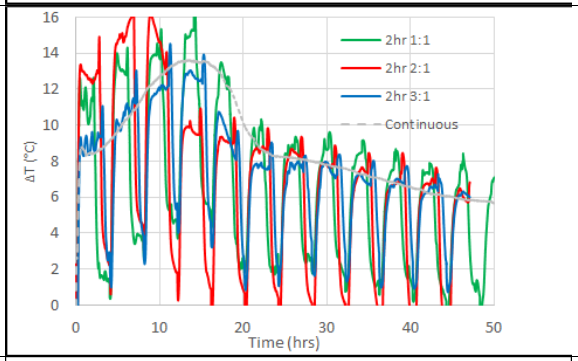	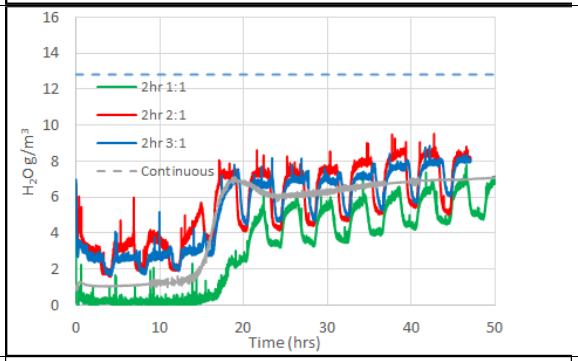
(iii) Position 2 - Mid reactor	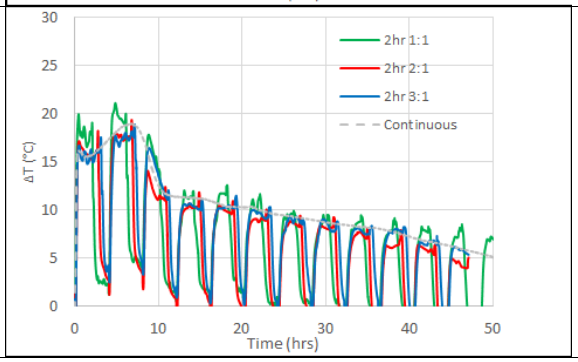	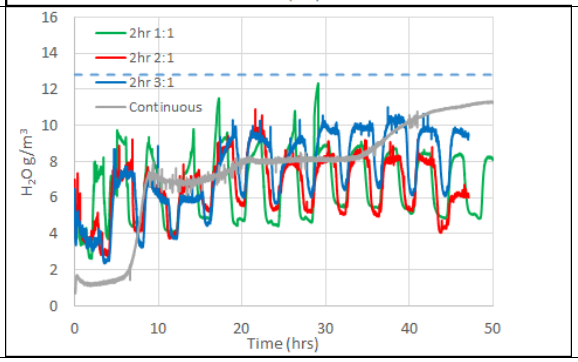

(iv) Position 1- (near inlet) of reactor

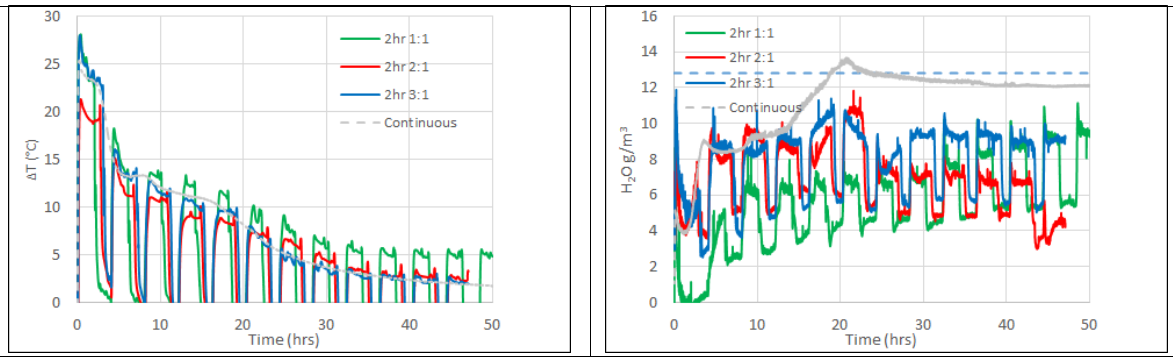

Figure 11 : The impact of moist air / dry air cycling at a switching interval of 2 hours on the temperature rise and air moisture level in the reactor. Each curve represents the proportion of wet : dry time during each cycle within a 2 hour cycle.

4. Discussion

The are a number of important issues which are raised by the investigation and its results. From examining the temperature and moisture profiles at the inlet (which are unhindered by upstream effects, Figure 7(a)iv)) it is possible to hypothesize on the mechanisms by which the $CaCl_2$ SIM is being hydrated, Figure 12 (a). It is proposed that the initial peak temperature rise is a result of the hydration reaction between the salt on the surface of the SIM. Immediately after the peak, there is plateau region region where the rate of energy liberation is limited by the diffusion of the water into the core of the porous SIM particle. This diffusion rate limiting reaction results in a steady reaction rate, reduced energy liberation and lower temperature. The SIM then undergoes steady cooling as the salt reactant is spent and the SIM accumulate additional water by deliquescence. Although Figure 12(a) depicts this as four distinct zones, there may be more than 1 hydration mechanism occurring, depending on the position within the SIM and the SIM particle size. This hypothesis is reinforced by the response of the $LiNO_3$ which undergoes a single hydrated state transition. A peak temperature spike is initially observed as the surface of the SIM is hydrated, followed by a plateau region where diffusion controls the energy liberation rate, Figure 12(b).

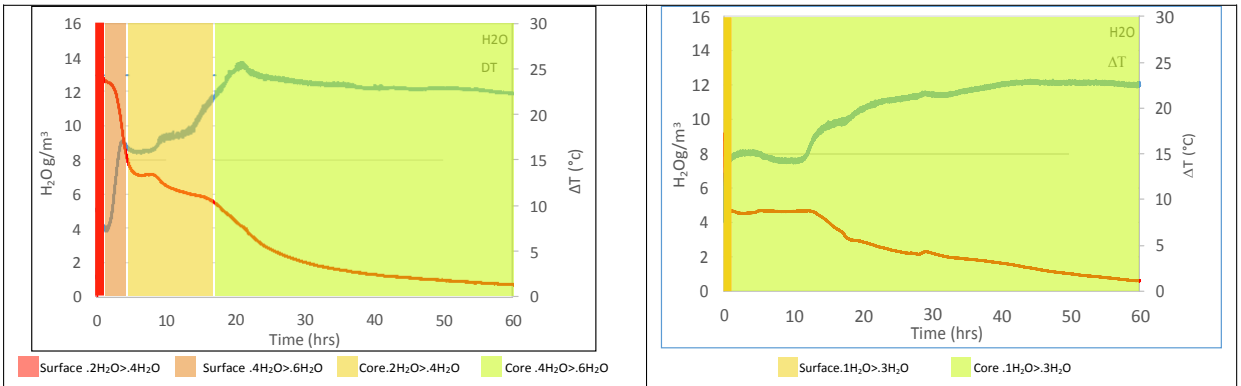

(a) $CaCl_2$ (b) $LiNO_3$

Figure 12 : Proposed mechanism of hydration of (a) CaCl2 vermiculite SIM where sufficient moisture is available.

From a material perspective it may be beneficial to lower the salt : vermiculite ratio and there is merit in further study at these lower salt : vermiculite ratios. This will reduce the theoretical energy storage density, but as this theoretical energy storage density is never achieved then the detriment

in real world performance may be negligible. Further improvement in performance may also be obtained by blending other salts such as $MgSO_4$ which benefit from hydration state changes within the temperature range and also have lower tendency to deliquesce, although they are not without other issues, [17,29,30].

The work has demonstrated that the behaviours of the $CaCl_2$ and $LiNO_3$ SIMs differ significantly between bulk material and single particle/thin layer (2-8 particles) geometries.. This has a significant impact on the potential performance of the technology . Limitations to scale arise as the area of deliquescence is typically only 60 – 100 mm into the bulk of the material from the edge. The deliquescence of the salt in the SIM means that penetration of moist air into the bulk is limited and thus has a detrimental effect on the performance of both $CaCl_2$ and $LiNO_3$ relative to an ideal performance. These laboratory findings have a direct impact on the design of a building scale energy storage system.

Building scale engineering solutions to this deliquescence include the design of a cartridge system where each section of material can be removed and replaced as the salt transitions from an energy liberating hydration stage to a energy sink deliquescence stage. Based on the findings of this study, this could be no more than 60 – 100 mm in depth. The physical layout of the reactor would also be redesigned such that there are multiple inlets to the bulk which will aid a more uniform distribution of the moist air into the SIM bulk. Modelling of reactor systems where the effective porosity of the medium changes with exposure to the air may be possible [31] and would potentially give a more rapid indication of improved designs.

This requirement for engineering complexity will impose additional cost and space penalties on any building scale storage system. The integration of the correct control measures through moisture and temperature measurement in the reactor will also need to be integrated with building BMS. Further work is on going by the authors on the development of both material and engineering solutions to the issues highlighted.

The results have an impact on reported energy densities where simple linear scaling is used to extrapolate real world energy densities from small sample laboratory results. Unless innovative reactor designs / operational solutions are developed, then it is likely that energy densities will be significantly overestimated/underachieved. Simple linear scaling from small sample laboratory measured energy densities to estimated building density capabilities are fundamentally flawed. The testing methodology developed which examines the SIM material at a packed density which is comparable to that which would be required in practice has shown itself to be a valid means of investigating potential SIM materials. It not only examines the thermodynamic potential of the material but also highlights practical issues which may be an obstacle to the implementation of the SIMs. The apparatus is currently being used to examine a variety of salt : matrix combinations, at a range of salt loadings.

5. Conclusions

A study of the potential capability of a building scale energy thermal storage system using salt hydration has been carried out. Laboratory studies carried out at high packing density found that the performance of the two SIM materials during the discharge cycle was significantly lower than that expected and that excess deliquescence of the salt material was found to the primary reason for this

under performance. Changes in the operation of the thermal storage reactor did little to do improve performance. The findings demonstrate that simple scaling rules cannot be used to estimate storage energy densities of building installations and that there will be a need to add significant complexity to a typical building installation.

Acknowledgements

The authors would like to thank EPSRC, Innovate UK, Welsh Government, ERDF and TATA Steel Colors for their support in this work.

References

[1] P. Tatsidjodoung, N. Le Pierr??s, L. Luo, A review of potential materials for thermal energy storage in building applications, Renew. Sustain. Energy Rev. 18 (2013) 327–349. doi:10.1016/j.rser.2012.10.025.

[2] A. Shukla, D.N. Nkwetta, Y.J. Cho, V. Stevenson, P. Jones, A state of art review on the performance of transpired solar collector, Renew. Sustain. Energy Rev. 16 (2012) 3975–3985. doi:10.1016/j.rser.2012.02.029.

[3] H.-Y. Chan, S.B. Riffat, J. Zhu, Review of passive solar heating and cooling technologies, Renew. Sustain. Energy Rev. 14 (2010) 781–789. doi:10.1016/j.rser.2009.10.030.

[4] C. Brown, E. Perisoglou, R. Hall, V. Stevenson, Transpired solar collector installations in Wales and England, Energy Procedia. 48 (2014) 18–27. doi:10.1016/j.egypro.2014.02.004.

[5] M.A. Leon, S. Kumar, Mathematical modeling and thermal performance analysis of unglazed transpired solar collectors, Sol. Energy. 81 (2007) 62–75. doi:10.1016/j.solener.2006.06.017.

[6] A. Sol??, X. Fontanet, C. Barreneche, I. Martorell, a. I. Fern??ndez, L.F. Cabeza, Parameters to take into account when developing a new thermochemical energy storage system, Energy Procedia. 30 (2012) 380–387. doi:10.1016/j.egypro.2012.11.045.

[7] J. Cot-Gores, A. Castell, L.F. Cabeza, Thermochemical energy storage and conversion: A-state-of-the-art review of the experimental research under practical conditions, Renew. Sustain. Energy Rev. 16 (2012) 5207–5224. doi:10.1016/j.rser.2012.04.007.

[8] L. Gordeeva, A. Grekova, T. Krieger, Y. Aristov, Composites “binary salts in porous matrix” for adsorption heat transformation, Appl. Therm. Eng. 50 (2013) 1633–1638. doi:10.1016/j.applthermaleng.2011.07.040.

[9] L. Scapino, H.A. Zondag, J. Van Bael, J. Diriken, C.C.M. Rindt, Sorption heat storage for long-term low-temperature applications: A review on the advancements at material and prototype scale, Appl. Energy. 190 (2017) 920–948. doi:10.1016/j.apenergy.2016.12.148.

[10] A.D. Pathak, S. Nedea, H. Zondag, C. Rindt, D. Smeulders, A DFT-based comparative equilibrium study of thermal dehydration and hydrolysis of $CaCl_2$ hydrates and $MgCl_2$ hydrates for seasonal heat storage, Phys. Chem. Chem. Phys. (2016). doi:10.1039/C6CP00926C.

[11] L.G. Gordeeva, Y.I. Aristov, Composites “salt inside porous matrix” for adsorption heat transformation: A current state-of-the-art and new trends, Int. J. Low-Carbon Technol. 7 (2012) 288–302. doi:10.1093/ijlct/cts050.

[12] K.E. N’Tsoukpoe, H. Liu, N. Le Pierr??s, L. Luo, A review on long-term sorption solar energy storage, Renew. Sustain. Energy Rev. 13 (2009) 2385–2396. doi:10.1016/j.rser.2009.05.008.

[13] S.P. Casey, D. Aydin, S. Riffat, J. Elvins, Salt impregnated desiccant matrices for “open” thermochemical energy storage - Hygrothermal cyclic behaviour and energetic analysis by physical experimentation, Energy Build. 92 (2015) 128–139. doi:10.1016/j.enbuild.2015.01.048.

[14] Y.I. Aristov, Challenging offers of material science for adsorption heat transformation: A review, Appl. Therm. Eng. 50 (2013) 1610–1618. doi:10.1016/j.applthermaleng.2011.09.003.

[15] D. Zhu, H. Wu, S. Wang, Experimental study on composite silica gel supported CaCl2 sorbent for low grade heat storage, Int. J. Therm. Sci. 45 (2006) 804–813. doi:10.1016/j.ijthermalsci.2005.10.009.

[16] I.A. Simonova, A. Freni, G. Restuccia, Y.I. Aristov, Water sorption on composite “silica modified by calcium nitrate,” Microporous Mesoporous Mater. 122 (2009) 223–228. doi:10.1016/j.micromeso.2009.02.034.

[17] S.P. Casey, J. Elvins, S. Riffat, A. Robinson, Salt impregnated desiccant matrices for “open” thermochemical energy storage - Selection, synthesis and characterisation of candidate materials, Energy Build. 84 (2014) 412–425. doi:10.1016/j.enbuild.2014.08.028.

[18] A.F. Lele, A Thermochemical Heat Storage System for Households: Thermal Transfers Coupled to Chemical Reaction Investigations, (2015). doi:10.1007/978-3-319-41228-3.

[19] J. Jänchen, H. Stach, Adsorption properties of porous materials for solar thermal energy storage and heat pump applications, Energy Procedia. 30 (2012) 289–293. doi:10.1016/j.egypro.2012.11.034.

[20] RCUK, INTRESTS RCuk site.pdf, INTRESTS - INterseasonal Thermochem. Renew. Energy Storage Syst. (2013). http://gtr.rcuk.ac.uk/projects?ref=101223 (accessed April 4, 2017).

[21] M. Molenda, J. Stengler, M. Linder, A. Wörner, Reversible hydration behavior of CaCl2 at high H2O partial pressures for thermochemical energy storage, Thermochim. Acta. 560 (2013) 76–81. doi:10.1016/j.tca.2013.03.020.

[22] K.E. N’Tsoukpoe, T. Schmidt, H.U. Rammelberg, B.A. Watts, W.K.L. Ruck, A systematic multi-step screening of numerous salt hydrates for low temperature thermochemical energy storage, Appl. Energy. 124 (2014) 1–16. doi:10.1016/j.apenergy.2014.02.053.

[23] K.E. N’Tsoukpoe, H.U. Rammelberg, A.F. Lele, K. Korhammer, B.A. Watts, T. Schmidt, et al., A review on the use of calcium chloride in applied thermal engineering, Appl. Therm. Eng. 75 (2015) 513–531. doi:10.1016/j.applthermaleng.2014.09.047.

[24] I. Simonova, Y. Aristov, Hydrates. or Storage O. Low Temperature Heat: Selection O. Promising Reactions and Nanotailoring O. Innovative Materials, Int. Sci. J. Altern. Energy Ecol. 10 (2007) 65–69. http://isjaee.hydrogen.ru/pdf/pdf/10-07/Simonova_65.pdf.

[25] L.G. Gordeeva, E.N. Moroz, N.A. Rudina, Y.I. Aristov, Formation of porous vermiculite structure in the course of swelling, Russ. J. Appl. Chem. 75 (2002) 357–361.

doi:10.1023/A:1016165915362.

[26] J. V. Veselovskaya, R.E. Critoph, R.N. Thorpe, S. Metcalf, M.M. Tokarev, Y.I. Aristov, Novel ammonia sorbents “porous matrix modified by active salt” for adsorptive heat transformation: 3. Testing of “BaCl2/vermiculite” composite in a lab-scale adsorption chiller, Appl. Therm. Eng. 30 (2010) 1188–1192. doi:10.1016/j.applthermaleng.2010.01.035.

[27] Y.I. Aristov, G. Restuccia, M.M. Tokarev, H.D. Buerger, A. Freni, Selective water sorbents for multiple applications. 11. CaCl2 confined to expanded vermiculite, React. Kinet. Catal. Lett. 71 (2000) 377–384. doi:10.1023/A:1010351815698.

[28] H. Wu, S. Wang, D. Zhu, Y. Ding, Numerical analysis and evaluation of an open-type thermal storage system using composite sorbents, Int. J. Heat Mass Transf. 52 (2009) 5262–5265. doi:10.1016/j.ijheatmasstransfer.2009.05.016.

[29] R.J. Sutton, J. Elvins, S. Casey, E. Jewell, J.R. Searle, The Optimsiation of Salt Impregnated Matrices as Potential Thermochemical Storage Materials ., ICNTREE 2015 17th Int. Conf. Nucl. Therm. Renew. Energy Eng. (2015).

[30] V.M. van Essen, H. a. Zondag, J.C. Gores, L.P.J. Bleijendaal, M. Bakker, R. Schuitema, et al., Characterization of MgSO4 Hydrate for Thermochemical Seasonal Heat Storage, J. Sol. Energy Eng. 131 (2009) 41014. doi:10.1115/1.4000275.

[31] F. Tariku, K. Kumaran, P. Fazio, Transient model for coupled heat, air and moisture transfer through multilayered porous media, Int. J. Heat Mass Transf. 53 (2010) 3035–3044. doi:10.1016/j.ijheatmasstransfer.2010.03.024.

Annexe 1 : Theoretical considerations for prediction of temperatures during the discharge phase.

The energy liberated by the hydration is given by :

$$E = m_s \Delta h_f \tag{A1}$$

Where m_s is the mass of the salt and the Δh_f is the enthalpy of formation difference between the final and initial hydrated state of the salt. This energy liberated raises the temperature of all the material in the reactor and the air passing through it. The total thermal mass is calculated as

$$\sum mC = m_s C_s + m_v C_v + m_r C_r + m_a C_a \tag{A2}$$

Where m and C represent mass and specific heat and the subscripts s, v, r and a refer to the salt, vermiculite, reactor body and air respectively. Vermiculite and salt masses are taken from the input material into the reactor. The reactor mass, including sensors, was calculated from dimensions and standard material properties for the relevant materials. Heat loss through natural convection from the reactor body was assumed to be zero. Although there will be some loss, this is a valid assumption as the relative indurative nature of the plastic reactor body provides insulation to the exterior atmosphere. The assumption that the entire body of the reactor is raised by the hydration reaction is almost certainly untrue and adds a compensating sink on the heat balance. Finally, experiments carried out with an flexible insulating covering also showed almost identical temperature profiles to those carried out without insulation. The expected temperature rise can then be derived from :

$$E = \Delta T \sum mC \tag{A3}$$

Using the constants from Table 1, constants from literature for the reactor body at a flow rate of 5 L/min and a air moisture level of 12.9 g/m^3 it is possible to show that the predicted temperature rise is 30 °C and 29 °C respectively.